Supporting Information (SI) Appendix

Cretaceous African life captured in amber

Alexander R. Schmidt, Vincent Perrichot, Matthias Svojtka, Ken B. Anderson, Kebede H. Belete, Robert Bussert, Heinrich Dörfelt, Saskia Jancke, Barbara Mohr, Eva Mohrmann, Paul C. Nascimbene, André Nel, Patricia Nel, Eugenio Ragazzi, Guido Roghi, Erin E. Saupe, Kerstin Schmidt, Harald Schneider, Paul A. Selden, and Norbert Vávra

Table of Contents

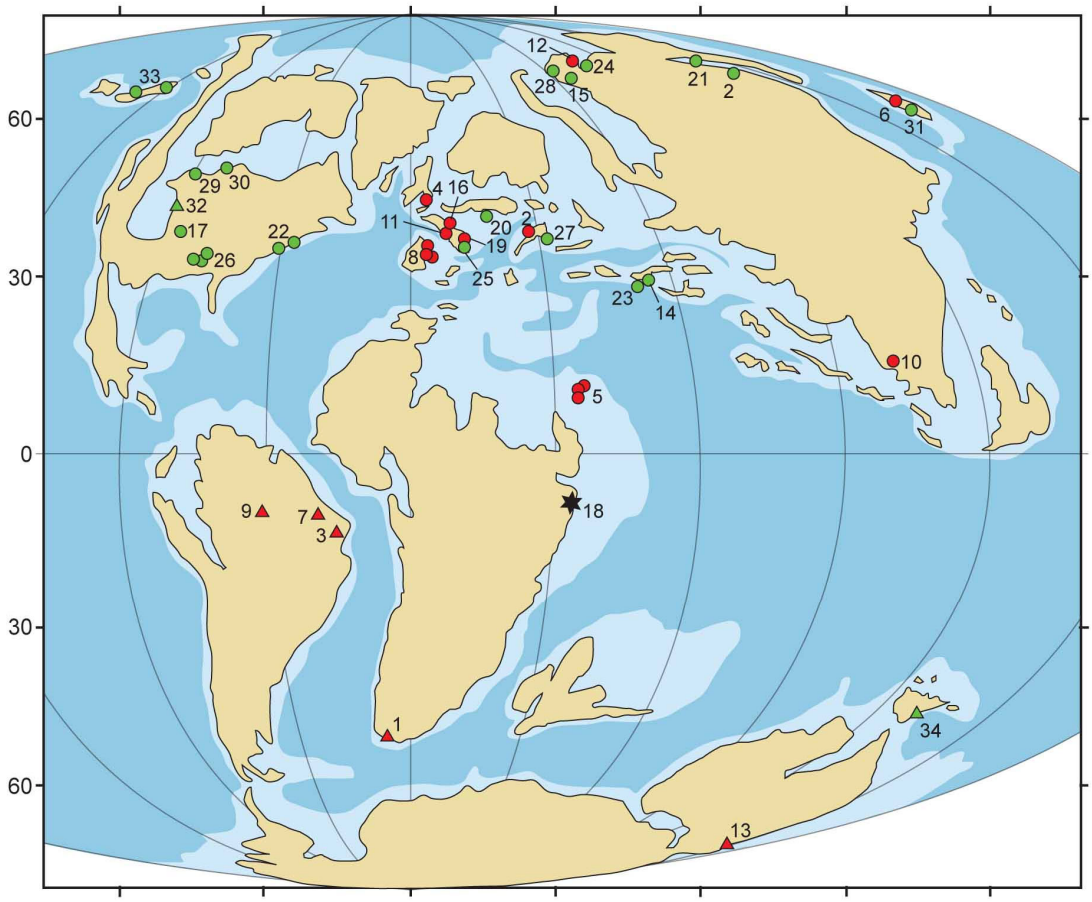

Fig. S1. Cretaceous amber deposits. Late Early Cretaceous map (ca 105 Ma) modified from Blakey (ref. 1); localities from Martínez-Delclòs *et al*. (ref. 2), with updates noted. Lower and Upper Cretaceous localities are symbolized in red and green, respectively. The Ethiopian amber is designated with a black star, circles represent amber localities that contain bioinclusions (mainly arthropods and/or microorganisms), triangles represent amber localities devoid of inclusions. (**1**) Kirkwood Formation, Eastern Cape Province, South Africa, Valanginian; (**2**) Golling, Austria, Hauterivian; (**3**) Maracangalha Formation, Recôncavo Basin, Brazil, Berriasian-Barremian (ref. 3); (**4**) Wessex Formation, Isle of Wight, U.K., Barremian; (**5**) "Levantine amber belt" (Lebanon, Jordan, Israel), Barremian-Aptian; (**6**) Choshi, Japan, Aptian; (**7**) Crato Formation, Araripe, Brazil, Aptian; (**8**) Escucha and Las Peñosas Formations (Peñacerrada, San Just, El Soplao), Spain, Lower Albian; (**9**) Alter do Chão Formation, Brazil, Albian (ref. 3); (**10**) Hukawng Valley, Myanmar, Upper Albian; (**11**) Charentes, France, Upper Albian and Lower Cenomanian (ref. 4); (**12**) Begichev Formation, Eastern Taimyr, Russia, Albian or Cenomanian; (**13**) Cape Paterson, Victoria, Australia, Lower Cretaceous; (**14**) Agdzhakend, Azerbaijan, Cenomanian; (**15**) Dolgan Formation, Agapa, Taimyr Peninsula, Russia, Cenomanian; (**16**) Ecommoy, Sarthe, France, Cenomanian; (**17**) Ellsworth County, Kansas, USA, Cenomanian; (**18**) Alem Ketema, Ethiopia, Cenomanian (this paper); (**19**) Salignac, France, Cenomanian; (**20**) Schliersee, Germany, Cenomanian; (**21**) Timmerdyakh, Yakutia, Russia, Cenomanian-Turonian; (**22**) U.S. Atlantic coastal plain (New Jersey, Maryland), Turonian; (**23**) Shavarshavan, Armenia, Coniacian; (**24**) Kheta Formation, Yantardakh, Taimyr Peninsula, Russia, Santonian; (**25**) Provence (Piolenc, Martigues, Belcodène), France, Santonian (refs. 4–6); (**26**) U.S. Gulf coastal plain (Alabama, Mississippi, Tennessee), Santonian (ref. 7); (**27**) Ajka, Hungary, Santonian-Campanian; (**28**) Baikura-Neru Bay, Taimyr Peninsula, Russia, Santonian-Coniacian; (**29**) Cedar Lake, Manitoba, Canada, Campanian; (**30**) Grassy Lake, Alberta, Canada, Campanian; (**31**) Kuji, Japan, Campanian; (**32**) Lance Formation, Wyoming, Maastrichtian; (**33**) Arctic Coastal Plain, Alaska, Upper Cretaceous; (**34**) Paparoa, New Zealand, Upper Cretaceous.

Geological Setting. The amber deposit was discovered about 9 km north-northwest of Alem-Ketema in the eastern part of the Northwestern Plateau of Ethiopia (Fig. 1). The outcrop is located on the slopes of the Wenchit River valley near the village of Midda, situated close to the Wenchit River bridge on the road from Alem-Ketema to Rema (Fig. S2). The amber pieces occur in a thin siltstone layer in the Debre Libanos Sandstone Unit. Several kilograms of amber have been recovered from the outcrop in the last eight years, of which about 1500 grams were accessible for our investigation.

The Mesozoic sedimentary succession of the Abay River (Blue Nil) Basin ranges from the Triassic to the Upper Cretaceous and comprises five lithologic units, including the Lower Sandstone Unit, the Gohatsion Formation, the Antalo Limestone Unit, the Mugher Mudstone Unit, and the Debre Libanos Sandstone Unit (8). This sedimentary sequence is covered by Eocene volcanics.

The marine Jurassic Antalo Limestone Unit is well dated by Foraminifera, ammonites and bivalves and ranges from the Callovian to the Kimmeridgian (8). In contrast, the virtual absence of age-diagnostic fossils in the Mugher Mudstone and Debre Libanos Sandstone Units has been emphasized in the literature (8, 9). These units form a regressive sequence. They probably represent the transition from a coastal to a continental fluviatile environment, in which marine index fossils are absent. The Mugher Mudstone Unit consists of supratidal to fluviatile sediments and the Debre Libanos Sandstone Unit is usually interpreted as a deposit of sandy braided rivers on a broad alluvial plain (8, 9). Vertebrate fossils and sporomorphs from the Mugher Mudstone Unit were studied by Goodwin *et al*. (10) and indicate an uppermost Jurassic (Tithonian) age for this unit. Bosellini *et al*. (11) revealed an unconformity between the Mugher Mudstone Unit and the Debre Libanos Sandstone Unit. These authors assumed an upper Barremian to Albian age for the Sandstone Unit. This estimation is based on a well-dated Lower Aptian marine horizon that the authors discovered in the lower part of the Upper Sandstone of the Harrar region in south-eastern Ethiopia. The precise stratigraphic range of the Sandstone Unit, however, remains uncertain. Some marine influence on the contemporaneous Amba Aradam Formation of northern Ethiopia is suggested (R.B., personal observation).

In general, most fossil resins were deposited in coastal, fluviatile to estuarine and shallow marine depositional environments where the resin pieces were reworked and accumulated from nearby coastal forests (e.g., refs. 12 and 13). Terrestrial influence on the amber-bearing siltstone deposit is evidenced by tiny wood remnants, spores and pollen grains. The occurrence of well-preserved vegetative stages of the exclusively limnetic conjugatophytes suggests close proximity to freshwater (Fig. S9 *A* and *B*), while dinoflagellate cysts of typical, shallow marine to brackish morphologies (Fig. S9*C*) suggest a coastal estuarine environment.

The age of the amber was estimated by a combined analysis of the physicochemical features of the amber, its inclusions and the sporomorphs of the amber-bearing sediment layer (see chapter *Amber Age Determination* of the *SI Appendix*).

Fig. S2. View of the steep slope exposing the Debre Libanos Sandstone Unit. The amber outcrop is shown by the red star. The location of the village of Midda is indicated by the arrow.

SI Materials and Methods. The physico-chemical properties of the amber were determined with respect to fluorescence under UV light, fracture, hardness, solubility in common solvents, and application of a hot point. Moreover, the amber was analyzed using fourier-transform infrared (FTIR) and thermal techniques [thermogravimetric analysis (TG) and differential thermogravimetric analysis (DTG)], gas liquid chromatography/mass spectroscopy (GLC-MS), and pyrolysis gas chromatography-mass spectrometry (Py-GC-MS). Solid-state fourier-transform infrared analysis was performed on freshly powdered samples of amber included in potassium bromide pellets. A Perkin Elmer system Spectrum BX FTIR Spectrophotometer was used in the wavelength range 2.5–15.5 μm (4000–645 cm^{-1}). TG and DTG patterns were obtained in the Institute of Geosciences and Earth Resources of the Italian National Council of Research (IGG-CNR, Padova, Italy, Aurelio Giaretta) by using a prototypal instrument, consisting of a platinum crucible, placed on a quartz glass support interfaced with a Mettler Toledo AB 104 balance. The heating rate was 10 K/min from room temperature to 700 °C. Analytical data were recorded by using software written in LabView 5.1 language, and thermal profiles edited using Grapher 2 software. Biomarkers ("chemofossils") were analyzed by treating the fossil resin with boiling chloroform to obtain a soluble fraction of the amber, which was then analyzed by means of gas liquid chromatography/mass spectroscopy. Classification and analysis of the macromolecular constituents of the amber was accomplished by pyrolysis gas chromatography-mass spectrometry analysis. Methodological details of these analyses are described elsewhere (14, 15), but briefly, the sample (~400 μg) is flash heated to 480 ^{o}C in the presence of excess tetramethyl ammonium hydroxide (TMAH) to methylate acidic products and the resulting pyrolysates are then analyzed by conventional gas chromatography-mass spectrometry. For this study, pyrolysis was carried out using a CDS 2500 Pyrolysis autosampler coupled with an Agilent 6890/5973 GC-MSD. Separation of pyrolysates components was achieved using a 60m ZB-1701 capillary GC column (250 μm id, 0.25 μm film thickness) using UHP He (1 mL/min constant flow) as carrier gas. Multiple analyses were performed and gave consistent results. For analysis of the hardness (HK) of the resin, five amber pieces were ground and polished on opposite sides using a Buehler Ecomet-3 variable-speed flat lap to produce two smooth, flat parallel / horizontal surfaces. A Leco Microhardness Tester with Knoop Indenter was set at a 500 g load level with a 10-second dwell time to test the hardness of each Ethiopian sample. Five to six individual indents were made on the uppermost horizontal surface of each piece tested. After averaging indent size for each sample, Knoop hardness (HK) was calculated: $HK = 14.229(F/D2)$, with F being the applied load (measured in kilograms-force) and D2 the area of the indentation (measured in square millimetres). This produced a hardness value for each sample, and these values were averaged. Comparison was then made to other Cretaceous fossil resins that are part of a larger study (see ref. 16 for preliminary results).

Extended Description of the Fossil Resin, with Remarks on Age-Relevant Information. ***Physico-chemical properties of Ethiopian amber.*** The studied samples were covered with a rough brownish crust (Fig. S3 *C* and *D*) and the inner color ranged from transparent light yellow to orange, with opaque areas (Fig. 2*B* and Fig. S3 *E*–*G*). The resin appears greenish and bluish in color when close to the surface of a piece and occasionally at fissures (Fig. S3 *F* and *G*). Under ultraviolet light (365 nm), the amber presents a weak yellowish fluorescence. The fracture is vitreous (Fig. S3*H*) and the specific gravity is about 1.10. Application of a hot point causes the amber to burn and emit a resinous odor. It is not soluble in ethanol, acetone or diethyl ether, tested by holding a small drop of solvent on the sample for 30 seconds and looking for any dissolution of the surface (this being a method of distinguishing between amber and other less mature resins; see ref. 17).

Fourier-transform infrared (FTIR) analysis of Ethiopian amber. The FTIR spectrum of Ethiopian amber is presented in Fig. S4, and it appears typical for a fossil resin. The first absorption band is at 2.9 μm (3500 cm^{-1}, marked as A in Fig. S4) and is due to the stretching of hydrogen–oxygen bonds (18, 19), such as phenolic and carboxylic hydroxyl functional groups. A part of these hydroxyl groups is probably responsible for the band, but it could also have resulted from water vapor contamination that occurred during the analytical procedure (18, 20).

The strong absorption near 3.4 μm (2950 cm^{-1}, band B in Fig. S4), here distinguishable as two bands, is caused by the stretching of aliphatic carbon–hydrogen bonds (18) and is considered diagnostic of resinous structures (19). Bending motions of the same structures produce an absorption peak near 6.8 μm (1470 cm^{-1}, band E) and 7.2 μm (1380 cm^{-1}, band F; ref. 18). The presence of a peak of intermediate intensity at 7.2–7.3 μm is considered assignable to CH_3 functional groups (19).

Another strong absorption band is detected near 5.8 μm (1700 cm^{-1}, band C), called the "carbonyl band" (18); it is also typical of all fossil resins and is caused by stretching movements of carbon–oxygen double bonds.

The above-described absorption bands are found in all fossil resins and therefore are not diagnostically interesting. The upper part of the infrared spectrum (i.e., higher than 8 μm) is difficult to interpret in terms of the specific chemical structure (18) because the vibrations are influenced by the carbon skeleton of the whole molecule. This region, however, is more useful than the lower region of the spectrum since it varies among the different resins. The region between 8 and 10 μm (1250–1000 cm^{-1}, G region in Fig. S4) presents absorption bands caused by carbon–oxygen single bonds (18, 21) and by aromatic ethers and phenols (19), and this region can be thought of as the fingerprint of a specific fossil resin (18). In this part of the spectrum, Baltic amber (also called *succinite* because of elevated content of succinates that act as cross-linking agents; concentration of free succinic acid is very low, as recently demonstrated by Tonidandel *et al*. (22)) exhibits the typical Baltic shoulder (see, for example, refs. 21 and 23–26), which consists of a single carbon–oxygen deformation band near 8.6–8.7 μm (about 1160–1150 cm^{-1}) preceded by a more or less flat shoulder between 8 and 8.6 μm (1250–1160 cm^{-1}). These deformation bands can be attributed to absorption of polyester-like structures (21, 27). The Ethiopian amber does not possess the characteristic Baltic shoulder and has only a very sharp peak at 8.6–8.7 μm; this is due to single carbon-oxygen bonds typical of the retinite group, which lacks succinic acid (25).

Absorption near 11.3 μm (885 cm^{-1}, band H in Fig. S4) is typical of out-of-plane bending movements of two hydrogen atoms in a terminal methylene group (18, 24) and may be attributed to resin acids (for example copalic and agathic acid). These acids are also found in recent resins, such as Madagascar copal, which is produced by species of the

genus *Hymenaea* (Leguminosae/Fabaceae family). Some true fossil resins, such as Mexican and Dominican amber (Oligocene–Miocene in age), also originating from the genus *Hymenaea* (28, 29), show a similar absorption band near 11.3 µm (30), although it is weaker in intensity because of the long resin maturation period. Ethiopian amber also peaks at 11.3 µm, but the peak is low in intensity, again reflecting long maturation time.

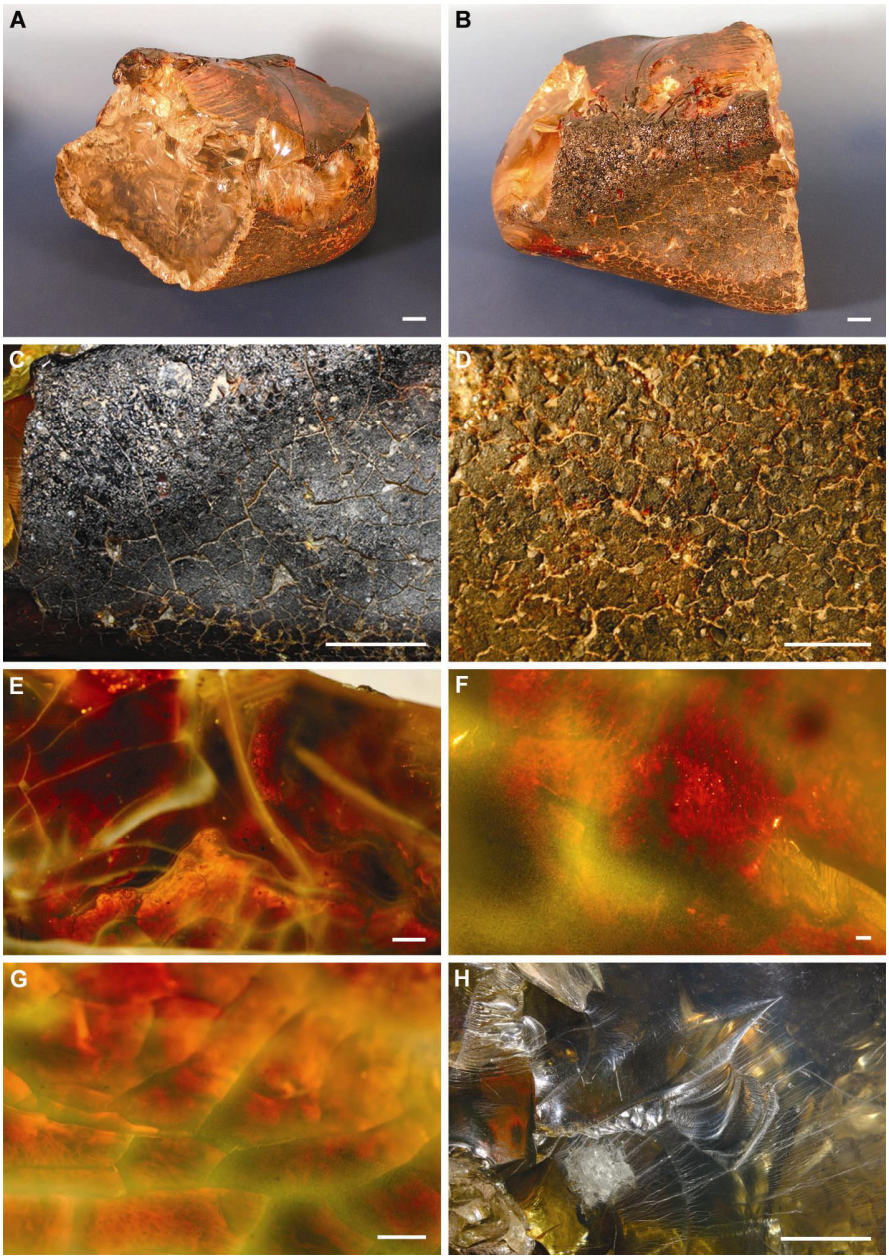

Fig. S3. Macroscopic features of the Ethiopian amber. (*A*, *B*) Additional views of the large translucent piece of amber of ca 1150 grams (NHMW, N3881). (*C*, *D*) Details of the amber surface with reticulate weathering marks (NHMW, N3881). (*E*–*G*) Color of the amber (MB. Pb. 2009/205). (*H*) Vitreous break surface (NHMW, N3881). [Scale bars: 1 cm (*A*–*D*, *H*), and 1 mm (*E*–*G*).]

Interestingly, the fingerprint region appears similar to that of resins from the *Agathis* genus (Araucariaceae), such as kauri gum (see spectrum in ref. 18, p.108, ref. 26, p. 94, and ref. 31, p. 43). Fossil kauri gum is believed to differ from succinite only in that it does not contain succinic acid, but the carbon skeleton is similar to that of succinite (31). Recent investigations using FTIR microspectroscopy (32) indicate that Baltic amber derives from conifers of the family Sciadopityaceae, and suggest that succinic acid and related compounds could reflect diagenetic alteration. The kauri resin contains bicyclic diterpenic acids of the labdane group but few abietic acid derivatives that are typical for *Abies* and *Pinus* genera. The Ethiopian amber spectrum is similar to that of gedanite (ref. 26, p. 79–81), which is a fossil resin of the retinite group that lacks the Baltic shoulder, of Lower Cretaceous Álava amber from Spain (33), which is attributed to an araucarian origin, and of Triassic amber from Dolomites, which has been suggested as possibly of cheiro-lepidiaceous origin (34).

An additional peak is found at 12.1 μm (band I in Fig. S4); assignment of peaks in the 12–14 μm region is only tentative (19) and thought to result from condensed aromatics or substitution in the benzene rings.

It is difficult to suggest a paleobotanical affinity for the fossil resin using only the infrared spectrum, also following the recent observations by Wolfe *et al*. (ref. 32). The chemical composition of fossil resins undergoes several changes during the process of resin maturation (i.e., amberization, ref. 35). The rate at which this process proceeds is strictly dependent on the temperature, age and thermal history of the sample. Therefore, resins with similar paleobotanical origins may present different compositions, as indicated by infrared spectroscopy. In summary, we show that infrared spectroscopy is a useful tool to characterize the polymer structures of this amber. Based on infrared spectroscopy, Ethiopian amber is unique and not identical to any type of fossil resin studied to date.

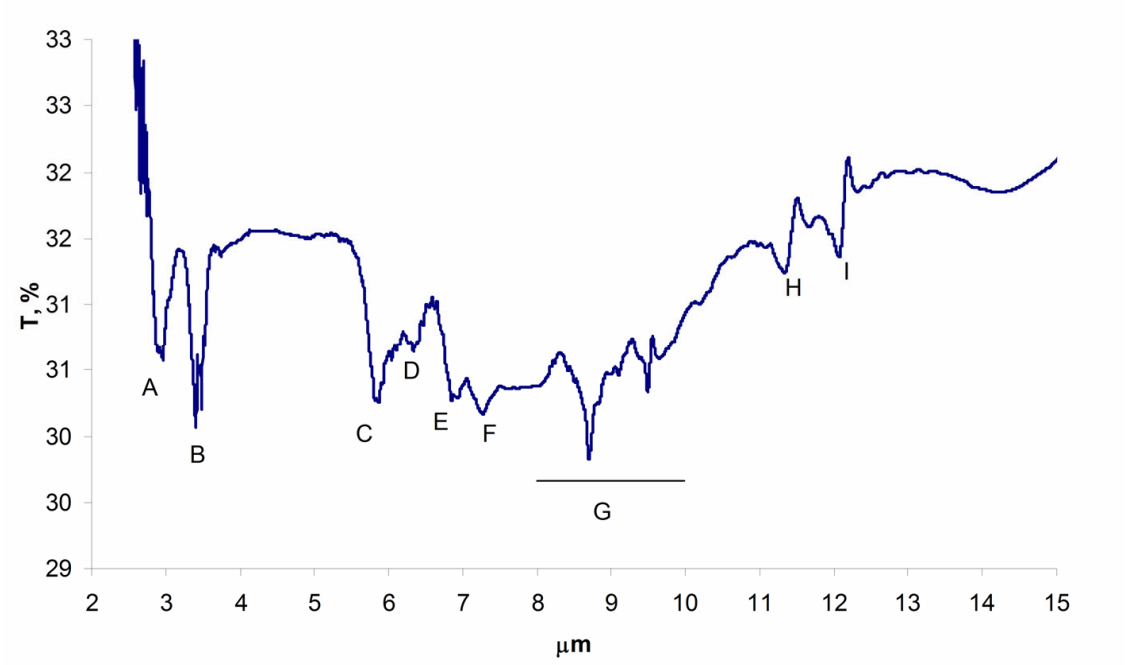

Fig. S4. FTIR spectrum of Ethiopian amber. The most relevant bands are indicated with letters and discussed in the text.

Thermogravimetric (TG) and Differential Thermogravimetric (DTG) analysis. Thermal analysis, namely thermogravimetric (TG) and differential thermogravimetric (DTG) analysis, has recently been applied to the study of fossil resins (36–38). Thermal analysis provides a rapid and quantitative method to examine the overall pyrolysis process and to estimate the effective rates of overall decomposition reactions, related to the chemical structure and degree of resin polymerization during the amberization process.

Ethiopian amber shows a TG combustion profile starting after 300 °C; total combustion occurred at about 600 °C (Fig. S5). DTG showed a main combustion event as a consequence of maximal rate of weight loss at about 430 °C (range from 429.5 to 433.5 °C). Another lower and broader peak was observed in the range 554–582 °C, with a maximum at 565–568 °C.

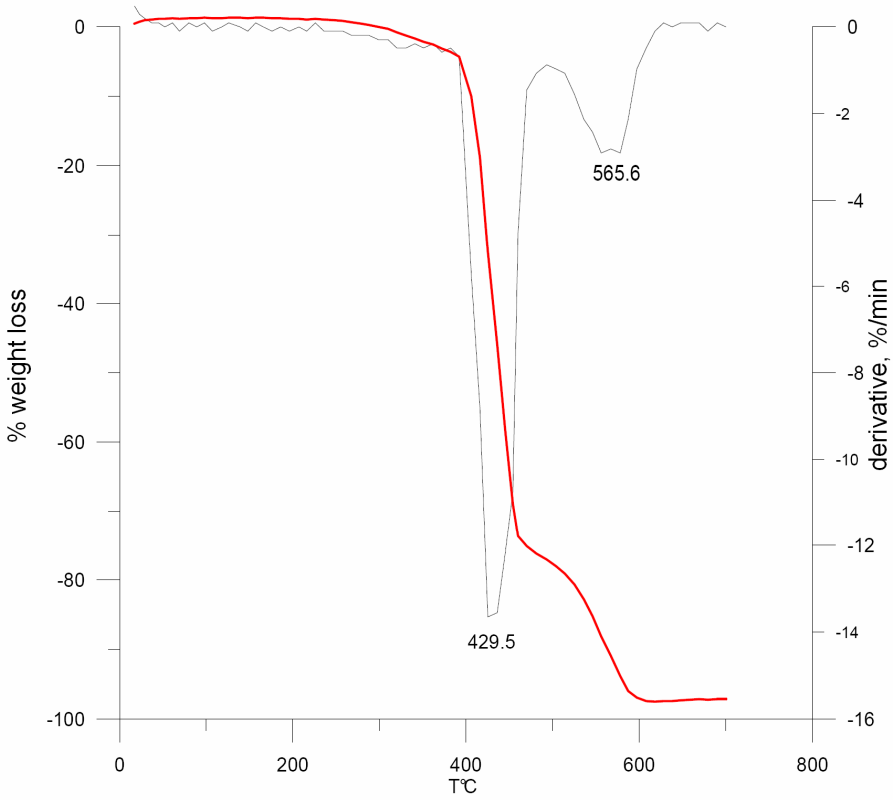

Fig. S5. Thermogravimetric (TG, red line) and Differential Thermogravimetric (DTG, thin line) analysis of Ethiopian amber.

According to published data (36, 37), the DTG main peak is proportional to the age of fossil resin and the degree of maturation. Comparison of thermal behaviour of Ethiopian amber with that of other fossil resins (37, 38) indicates that the main thermal peak may correspond to an age of about 110–120 Ma (Aptian-Albian, Fig. S6).

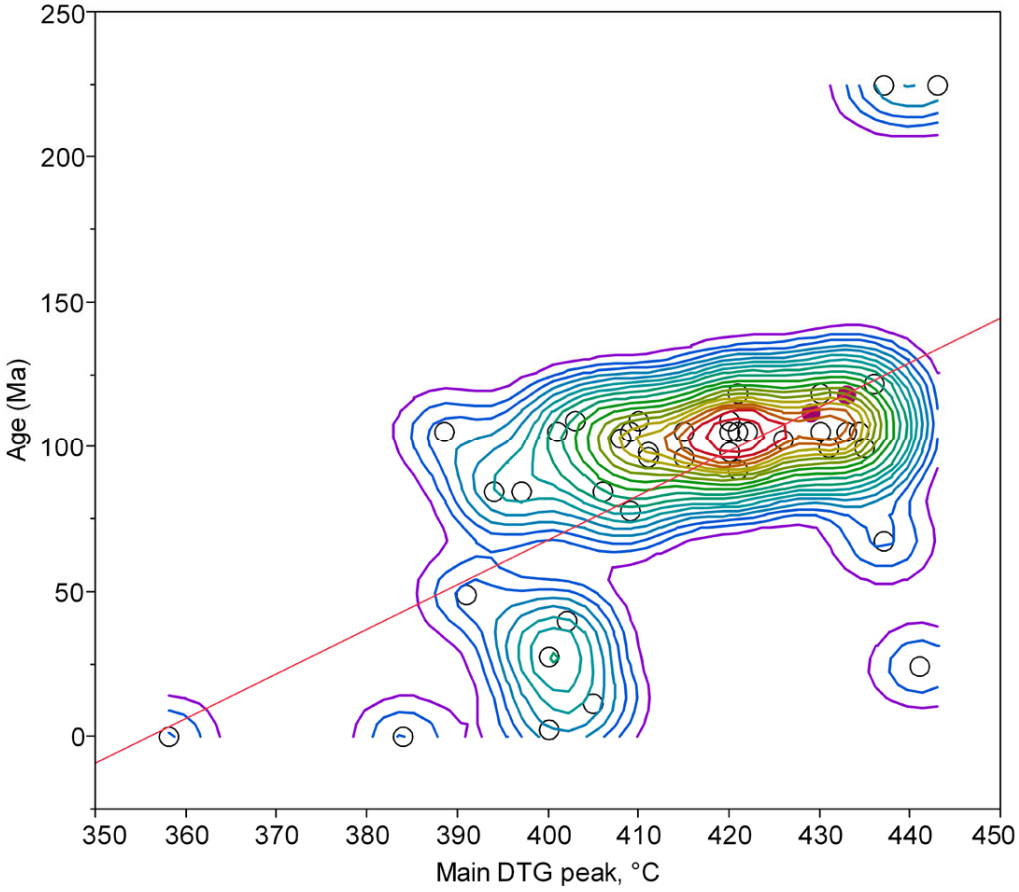

Fig. S6. Plot of Main DTG peak in relation to age of amber as previously determined in samples of different ages and provenances (see refs. 37, 38). The density map with contours at quantiles is also reported. The Main DTG values obtained with samples of Ethiopian amber are indicated with red dots. According to the linear correlation (red line), the geological age of the amber was estimated to be 110–120 Ma (Aptian-Albian).

Gas liquid chromatography/mass spectroscopy. The chemofossils show characteristics typical of Mesozoic amber: (1) a low total amount of low molecular weight substances, (2) a high degree of diagenetic influence on molecular structure, and (3) a very small amount of original terpene structures. More than 42 percent of the investigated substances correspond to compounds that are already known from other Mesozoic resins.

A soluble fraction of the amber, obtained by treating the resin with boiling chloroform, was analyzed by means of gas liquid chromatography/mass spectroscopy. The amount of soluble compounds obtained was extremely low, and thus only a few tentative identifications of single compounds could be made. Mass spectra from different ambers were compared, however, and focused on more than 20 peaks as a way of "fingerprinting" the ambers and comparing the compounds. Six of the peaks showed striking similarities and even identity with compounds found in other Mesozoic ambers, especially with a still undescribed amber sample from the Jurassic of Jordan (material obtained from Klaus

Bandel, University of Hamburg). Taken together, these substances comprise more than 30 percent of the area of all the observed peaks.

Tentative identifications: (1) α-pinene (small traces only), (2) bornylene or limonene (6 area %), (3) 2-(1,1-dimethylethyl)-phenol, (4) terpene, possibly camphor (16 area %), (5) trimethyltetraline or: tetramethyl-2,3-dihydroindene (18 area %), (6) pentamethyl-2,3-dihydroindene (11 area %), (7) possible caryophyllene alcohol (8 area %), (8) unidentified aromatic compound (16 area %), and (9) possibly a bicyclic sesquiterpene (mol. mass: 222; approx. 7 area %).

Results achieved can be summarized as follows: (1) The content of soluble compounds is extremely low; (2) more than 45 (area) % of substances studied are aromatic compounds; this fact seems to indicate a rather high degree of diagenetic change – due, for instance, to the high geological age or, possibly, to tectonic events; and (3) only a few substances show the original terpene structures. Unfortunately, however, none of the substances can be used as a reliable 'biomarker' to suggest a possible botanical source for this amber.

It is worth mentioning that Roghi *et al*. (34) detected possible traces of camphor (its structure is very similar to the bornylene mentioned above) and a number of aromatic compounds by means of pyrolysis gas chromatography in Triassic amber from Italy.

Pyrolysis gas chromatography-mass spectrometry (Py-GC-MS). Typical results of the pyrolysis gas chromatography-mass spectrometry are illustrated in Fig. S7 below. The structures of identified components of the pyrolysates are illustrated in Fig. S8.

Chemical analysis of the Ethiopian amber indicates it is a mature Class Ic amber; this is the first Class Ic amber ever reported from the Cretaceous. The majority of the products observed are bicyclic products derived from the A/B ring system of the original labdanoid precursors. Based on retention characteristics and comparison with characteristic products derived from previously investigated ambers, the products derived from these samples are based on so-called *enantio*-series labdanoids, including ozic acid, ozol and *enantio*-biformene. The pyrolysates also contains a high proportion of products derived by defunctionalization (5–8 and 13–16) or aromatization (10, 12, 19 and 20) of the original labdanoids and lacks significant occluded low molecular weight products, consistent with a moderately high level of maturity.

Although we don't have conclusive information regarding its botanical source, conceivably the resin could have been produced by a previously unknown Cretaceous gymnosperm, or possibly even from a mid- to late-Cretaceous angiosperm. Its chemistry is analogous to that of less mature Miocene angiosperm ambers found in Mexico and the Dominican Republic that were produced by members of the genus *Hymenaea* (39). Surprisingly, Late Carboniferous Illinois amber was also recently determined to be a Class Ic resin (40), derived from an unknown plant, possibly an early gymnosperm.

Chemical evidence suggests that the Ethiopian amber was not produced by representatives of the Cheirolepidiaceae, despite the presence of pollen grains of this Mesozoic conifer family in the amber-bearing sediment. Recent chemical analysis of a known Cheirolepidiacean amber from the Late Triassic of northern Italy (34) indicates that the Italian resin has a distinctly different macromolecular structure and is, in fact, a Class Ib amber.

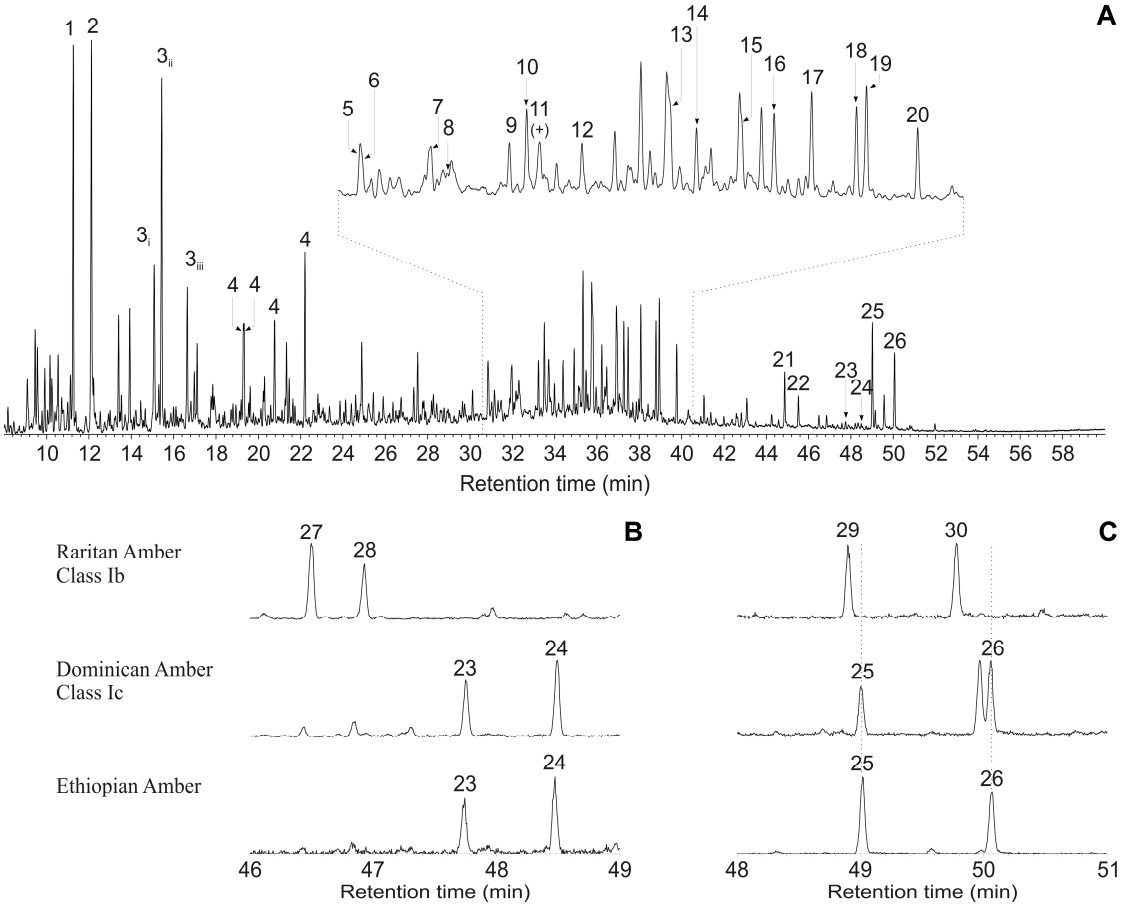

Fig. S7. Py-GC-MS data from analysis of Ethiopian amber. (*A*) Total Ion chromatogram, showing the distribution of products observed in the pyrolysate of this sample. Numbering corresponds to structure key illustrated separately as Fig. S8. (*B*) Reconstructed Ion Chromatogram (RIC) (m/z=248 + 250), showing observed distribution of characteristic C_{15} bicyclic acids observed in Ethiopian amber. (*C*) RIC data (m/z=220 + 222) showing observed distribution of characteristic C_{15} bicyclic alcohols observed in Ethiopian amber. For both (*B*) and (*C*), RIC data for known reference ambers from the Dominican Republic (Class Ic, ref. 41) and Raritan formation of the Atlantic Coastal Plain (Class Ib, ref. 15) are included for comparison. Based on these data, this amber is identified as Class Ic.

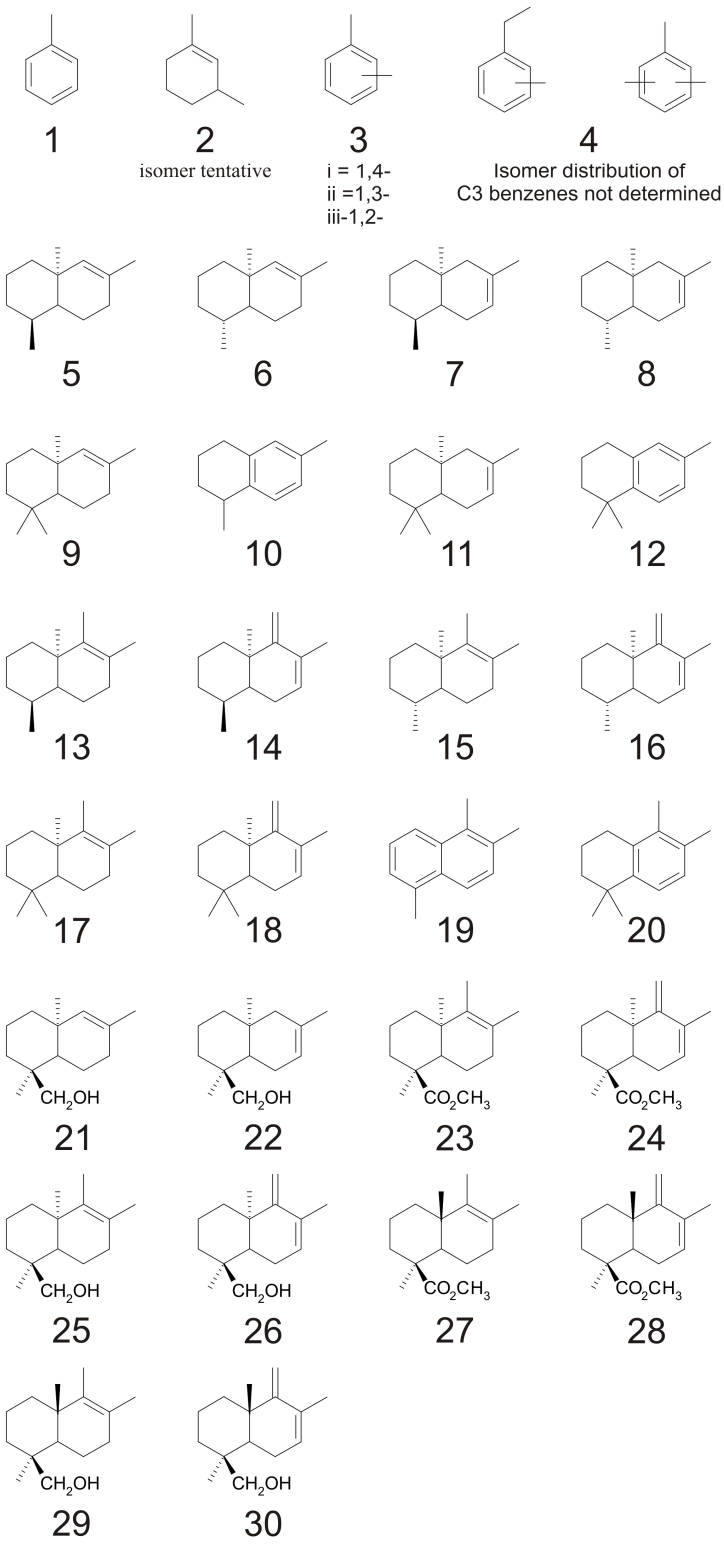

Fig. S8. Structure key illustrating structural characteristics of products identified in the pyrolysates of Ethiopian amber. Numbering of individual products corresponds to numbering of peaks indicated in Fig. S7.

Indentation Hardness (HK). Using a Knoop Hardness Indenter, we obtained the following indentation hardness (HK) values for the five Ethiopian amber samples analyzed: 15.2, 14.8, 14.7, 13.2, and 13.2. The overall HK value is 14.22.

The Ethiopian amber appears to fall within the expected hardness range for mature Upper Cretaceous Class I fossil resins; however, the Class Ic designation for this amber is unique among known Cretaceous resins, so further study and comparison with other Cretaceous ambers is needed.

Palynomorphs of the Amber-Bearing Sediment. The organic matter obtained from the amber-bearing siltstone is relatively mature and consists of nearly 100% of shredded terrestrial plant material. The palynoflora is dominated by various fungi, mosses, lycophytes and ferns as well as gymnosperms. Fungal spores are particularly abundant, especially the genera *Fusiformisporites* (Fig. S9*D*) and *Pluricellaesporites* (Fig. S9*E*). Both taxa are common in the Mesozoic and Cenozoic and thus are not stratigraphically informative. Additional taxa comprise verruculose conidia of dematiaceous hyphomycetes with two to three septae (Fig. S9*F*) and small *Lycoperdon*-type spores with variable spines (Fig. S9*G*); they range from the Cretaceous to the recent (42). Spores of ferns are rare, and only a few types have been found. Nobby monolete *Cryptogramma*-type spores (Fig. S9*H*), smooth trilete *Dickinsonia*-like spores and pteridaceous spores of the genus *Polypodiaceoisporites* (Fig. S9*I*) have been found; all of these were common during the Cretaceous. *Cicatricosisporites*, a schizaeaceous spore type that is generally most common during the Late Jurassic to mid Cretaceous, *Baculatisporites* (Fig. S9*J*), as well as *Cyathidites* cf. *punctatus* and other *Cyathidites* taxa occur in the sediment. Among several conifer pollen taxa, lumps of *Corollina* are recognizable (Fig. S9*K*). This pollen type derived from the extinct Mesozoic conifer family Cheirolepidiaceae and is common from the Triassic through the Lower/mid Upper Cretaceous. Angiosperm pollen taxa include a triporate type, *Triorites* sp. (Fig. S9*L*), which is possibly related to Proteales and close in appearance to *Triorites africaensis*, but with a clear reticulum. *Triorites africaensis* is a marker for the late Cenomanian in Central to eastern Africa (43). An additional pollen type (Fig. S9*M*) seems to belong to early members of the Normapolles complex (?*Oculopollis*), a group that is known to range from the mid/Late Cenomanian through the Paleogene (44). A tricolpate pollen type (Fig. S9*N*) with an unusual morphology may belong to a Cretaceous East African taxon that has not yet been described.

In conclusion, the sporomorph spectrum is unusual because it is dominated by fungal remains. Spores and pollen do not include index fossils; however, because of the appearance of common Cretaceous fern taxa and an angiosperm flora that includes early Normapolles and possibly early protealean taxa, an early Upper Cretaceous age (Late Cenomanian) is most likely. In eastern Africa, pollen spectra of Coniacian to Santonian age are dominated by tricolpate and tricolporate taxa and are characterized by the genus *Droseridites* (45), features that have not been observed in this Ethiopian assemblage.

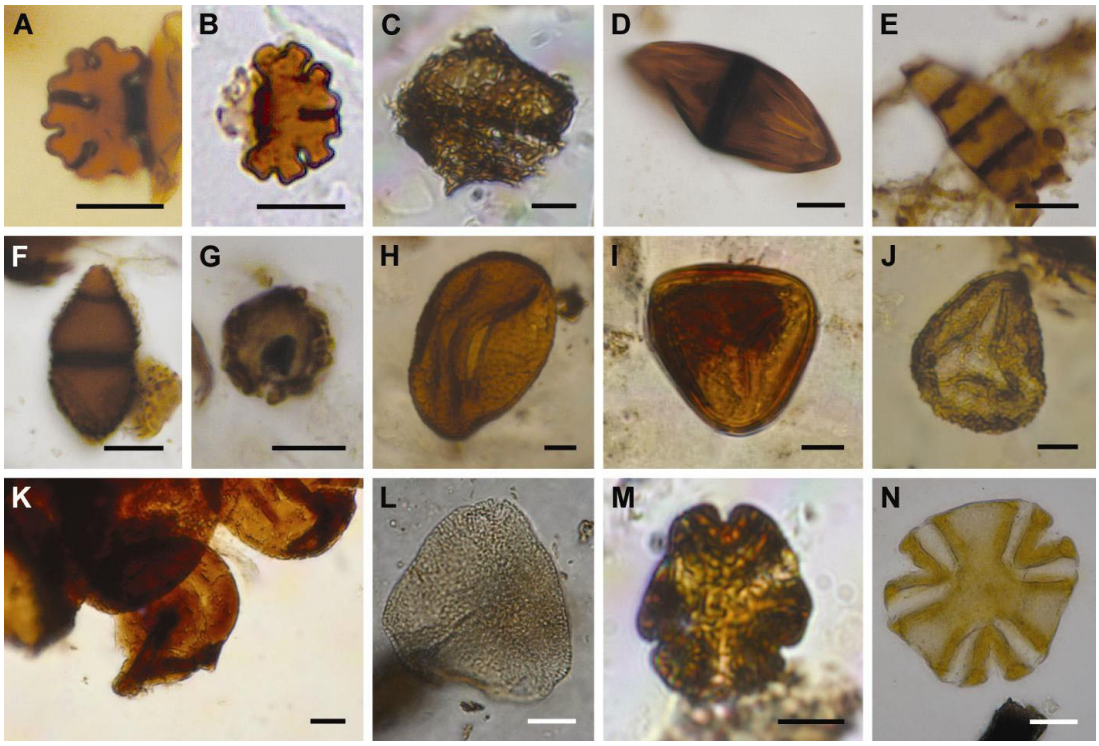

Fig. S9. Relevant palynomorphs of the amber-bearing sediment. (*A*, *B*) Half cells of a *Cosmarium*-like conjugatophyte. (*C*) Possible cyst of a dinoflagellate. (*D*) *Fusiformisporites*. (*E*) *Pluricellaesporites*. (*F*) Verruculose conidia of dematiaceous hyphomycetes. (*G*) *Lycoperdon*-type spores (puff balls). (*H*) Nobby monolete *Cryptogramma*-type spore. (*I*) *Polypodiaceoisporites*. (*J*) *Baculisporites*. (*K*) *Corollina*. (*L*) *Triorites* sp. (*M*) Representative of the Normapolles complex. (*N*) Undetermined tricolpate pollen type. (Scale bars: 10 µm.)

Amber Age Determination. The age of the Debre Libanos Sandstone Unit has only been estimated in the literature. Thus, we used independent sources to date the amber. Apart from the stratigraphic range of the sporomorphs of the sediment, we obtained age-relevant information from the physicochemical properties of the amber itself (thermogravimetric and hardness analyses; see chapter *Extended description of the fossil resin* of the *SI Appendix*) and from its inclusions. Based on the palynological analysis, the amber-bearing siltstone is likely Cenomanian in age (see chapter *Palynomorphs of the amber-bearing sediment* of the *SI Appendix*). The occurrence of the genus *Triorites* and early Normapolles as well as the lack of characteristic late Upper Cretaceous angiosperm pollen (e.g., palm pollen) makes a younger age very unlikely. Hardness analysis also suggests an Upper Cretaceous age. Finally, most insect inclusions possess characters in accord with an early Upper Cretaceous age. The amber might be slightly older than Cenomanian since the differential thermogravimetric analysis suggests an Aptian-Albian age. When allowing for possible redeposition of the amber from older (pre-Cenomanian) sedimentary deposits, the maximum age of the amber is limited to the Upper Aptian by the angiosperm cuticle of the Lauraceae or Chloranthaceae or Proteaceae family inside the resin (Fig. S12*C*). We consider a late Lower Cretaceous age to be unlikely, however, since ambers found within a single, plentiful deposit are usually not much older than the sediment it contains. Fossil resins do not survive high-energy processes of erosion, transport and redeposition very

well, and reworking of amber-containing sediments by rivers or the sea would disperse and/or distribute the resin pieces so that a Lagerstätte would be unlikely to form secondarily. The large number of delicate amber pieces also supports *in-situ* deposition. In summary, combined analysis of these physicochemical and biological parameters indicates a Late Cenomanian age (ca 93–95 million years old) for the amber.

Additional Description of the Inclusions of Arthropods, Microorganisms and Plant Remnants. ***General remarks.*** Prior to the discovery of the Ethiopian deposit, African amber was known only from small, inclusion-less pieces from the Upper Triassic Molteno Formation of Lesotho (46) and from the Lower Cretaceous Kirkwood Formation of South Africa (47). Often confused with true amber, copal from Madagascar and Tanzania is a much younger resin with ages of only several hundreds to many thousands of years (48); arthropod inclusions described from copal are identical or very close to modern animals and therefore not very informative on ancestral lineages and ancient ecosystems. The fossiliferous amber deposits closest to the Ethiopian locality are from the Lower Cretaceous of Lebanon, Jordan and Israel, sometimes referred to as the "Levantine amber belt" (49). Coniferous trees of the Araucariaceae (50) and Cheirolepidiaceae (51, 52) are assumed to be the source of that amber. There are a few other Gondwanan ambers known from Brazil, Australia and New Zealand, which most likely do not contain inclusions, and only a handful of pieces were found at each locality (53).

Fossil insects preserved as impressions in sediments are similarly rare in the Cretaceous of Africa. The only abundant deposit is from the Turonian of Botswana (54) and a very few, isolated discoveries are mentioned from four localities in Algeria, Egypt, and Tunisia (55, 56).

Tree resin acts as an instant trap for arthropods. As a consequence, amber is usually an exceptional medium in which organisms can be exquisitely preserved, e.g. with their initial volume, minute structures, and sometimes even with colors. Arthropods inside the Ethiopian amber, however, are largely preserved more or less flattened, with translucent or darkened cuticle, indicating diagenetic alteration. This suggests that the arthropods were possibly dead and deteriorated before entombment in the resin or desiccated after entombment. Therefore, study of these inclusions is often difficult, despite the translucence of the amber.

The resin of the Ethiopian amber forest probably flowed or dropped into various terrestrial habitats. Arthropods flying or crawling along tree bark as well as dwellers of forest floor litter are preserved in the amber. Aquatic organisms are absent in the amber pieces.

Thysanoptera. Two thrips have been found, but only one nearly complete female specimen shows enough characters to be assigned to a family (Fig 3*C*, see also Fig. S10*C*). The attribution to the Merothripidae is based on the observed 8-segmented antennae, with the third and fourth segments with inflated placoid sensilla occupying a large area at the apex; the very narrow fore wings with the veins lying close together; and a pair of large sensoria on the tenth abdominal tergite, each with a long axial seta (trichobothria, ref. 57). *Jezzinothrips* Strassen 1973 (Upper Cretaceous Lebanese amber), putative oldest record of this family, was first described as a member of the heterothripoids (58) and only afterwards its family, Jezzinothripidae Strassen 1973, was synonymized with Merothripida. This was done without further examination of the fossil and without convincing argument (59). The only other mention of fossil merothripids are from Eocene Baltic amber and Miocene Mexican amber (60, 61).

Araneae. We tentatively assign the spider to the family Linyphiidae. Linyphiid synapomorphies were enumerated recently by Arnedo *et al*. (62). These include: on the male palp, presence of a suprategulum, absence of the araneid median apophysis and conductor, and presence of the radix in the embolic division. Synapomorphies that diagnose linyphiids and their sister family, the pimoids, are: sparse setae on the carapace, an intersegmental paracymbium on the male palp, presence of stridulatory ridges on the chelicera, patella-tibia autospasy, enlargement of the mesal cylindrical gland spigot base on the female posterior lateral spinnerets, and a sheet web. The morphological characters are difficult to see on the fossil because it is shriveled by dehydration (a common phenomenon which also afflicts modern spiders and hinders identification). However, the habitus (long, thin legs, ovoid opisthosoma and eye pattern, Fig. 3*B*) is typical of linyphids and pimoids. Three legs on the fossil are missing, the distal part of the leg from the tibia onwards, which suggests autospasy at the patella-tibia joint, a common reaction in a trapped spider. The conformation of the male palp of the fossil is clearly linyphiid or pimoid, and the intersegmental paracymbium is sickle-shaped, which is typical of many linyphiine genera, and would thus suggest Linyphiidae rather than Pimoidae. Furthermore, the specimen appears to lack the pimoid male palpal synapomorphies of a retrolateral cymbial sclerite and a dorsoectal cymbial process.

Lepidoptera. The presence of lepidopterans in the Ethiopian amber forest is evidenced by microscopic scales (Fig. S10*F*) that usually cover their wings and body. The scales are elongate and possess the characteristic array of parallel grooves observed in all lepidopteran scales, but it is not possible to assign them to any family based on these characters alone.

Coleoptera. We found two coleopteran fragments (NHMW, N6967e and NHMW, N6983c, which are fragments of one original amber piece), which likely belonged to a single beetle, but a more specific placement is not possible based on these remnants alone. There is a complete stout leg with five tarsomeres conspicuously enlarging towards the apex (Fig. S10*H*), as well as a fragmentary head comprising a geniculate, 11-segmented antenna with the flagellum distinctly enlarged towards the apex and the right mandible with four teeth along the inner margin (three small ones and a larger, apical one; Fig. S10*I*).

Psocoptera. Two specimens have been found but are not identifiable since they are the wingless larval stages and their poor preservation does not allow for the observation of critical features (Fig. S10*B*).

Hemiptera. Assignment of one specimen to the Aleyrodoidea is only tentative, based on wing venation and morphology of the legs and antennae. Most of the body is too damaged for a clear observation of diagnostic characters (Fig. S10*D*). A larva is also identified as an undetermined Hemiptera based on the presence of a small rostrum (modified mouthpart) visible ventrally and the general hemipteran-like morphology (Fig. S10*E*). At this stage there are not enough visible features for a more precise identification.

Zoraptera. The specimen is a complete, wingless individual apparently not deformed but with translucent cuticle (Fig. 3*E*). Visible diagnostic characters for this order include the legs with two-segmented tarsi, the basal one being greatly reduced with an enlarged hind femora, and a nine-segmented antennae. It is not clear if there is a mating hook or not. The most striking feature is the absence of stout spines along the hind femur and tibia, which could distinguish it from the only known genus *Zorotypus*.

Collembola. Five springtails have been recognized, four of which are fragmentary or too poorly preserved to be assigned to any family, but they show the characteristic abdominal furca that allow springtails to propel themselves into the air (Fig. S10*A*). The more complete specimen may belong in the Isotomidae based on its elongate body, globular

head, the broad first antennal segment, and several long, erect setae on the dorsal segments of the thorax and abdomen (Fig. 3*D*).

Diptera. We found fragments of three identical legs that we tentatively attributed to a dipteran, although the family cannot be identified (Fig. S10*G*). These are long, slender legs with only the tibiae and five cylindrical tarsomeres preserved; the first tarsomere is the longest, the second to fifth being subequal in length, and with very small tarsal claws. This morphology is most commonly encountered in dipterans.

Hymenoptera. *Trichogrammatidae*. This family of small parasitic wasps is characterized by the following combination of characters visible in our fossils: tarsi three-segmented, with first tarsomere the longest; the forewing with postmarginal vein absent, with setae arranged in radiating lines; and the metasoma widely attached to the mesosoma (see Fig. 3*I*). Trichogrammatids are divided into two subfamilies distinguished on the basis of the male genitalia (63), which is poorly visible, and therefore we cannot make any further designation.

Mymaridae. Six inclusions are identifiable as mymarid wasps, three of which are nearly complete while the others are more fragmentary. The two best-preserved ones (Fig. 3*G* and Fig. S10*J*) are females characterized by eight or ten-segmented antennae with a distinct club, narrow, paddle-like wings with long marginal hairs, legs with five tarsomeres, and a widely attached metasoma. The third well preserved individual (Fig. S10*K*) is a wingless (dealate?) male with an 11-segmented antennae, legs with five tarsomeres, and a metasoma widely attached to the mesosoma.

Mymarommatidae. One minute wasp belongs to this family based on highly distinctive features, including the forewing membrane with a mesh-like pattern and long marginal hairs, a reduced hind wing to an apically bifurcate haltere-like structure, a petiole composed of two tubular segments, and the antenna with four apical segments forming a compact tube (Fig. 3*H*).

Eulophidae. A small wasp can be attributed to this family based on the characteristic legs with only four tarsomeres, the reduced wing venation, a small, straight protibial spur (as opposed to the larger, curved one in most other chalcidoids), and by the antennae with less than ten antennomeres (seven) and a four-segmented funicle (Fig. 3*F*).

Formicidae. A single wingless female, i.e., a worker, has been found (Fig. 3*A*). The specimen is complete but enrolled, which makes it difficult to study. A virtual 3D reconstruction using phase contrast X-ray synchrotron imaging is currently being performed at the European Synchrotron Radiation Facility using the methodology developed for amber inclusions by Tafforeau *et al*. (64) and Lak *et al*. (65). This will elucidate characters and allow for the identification of this important fossil. Nevertheless, a few characters are clearly visible, including large, triangular to falcate mandibles with at least nine large teeth along the inner margin and a very long scape (longer than the head height). This precludes affinities with the extinct, widespread Cretaceous subfamily Sphecomyrminae, and instead suggests a worker ant with characteristics of modern groups. This is the oldest record of an ant from Gondwana, the only other fossils being three genera of uncertain subfamily from the Turonian of Botswana (66).

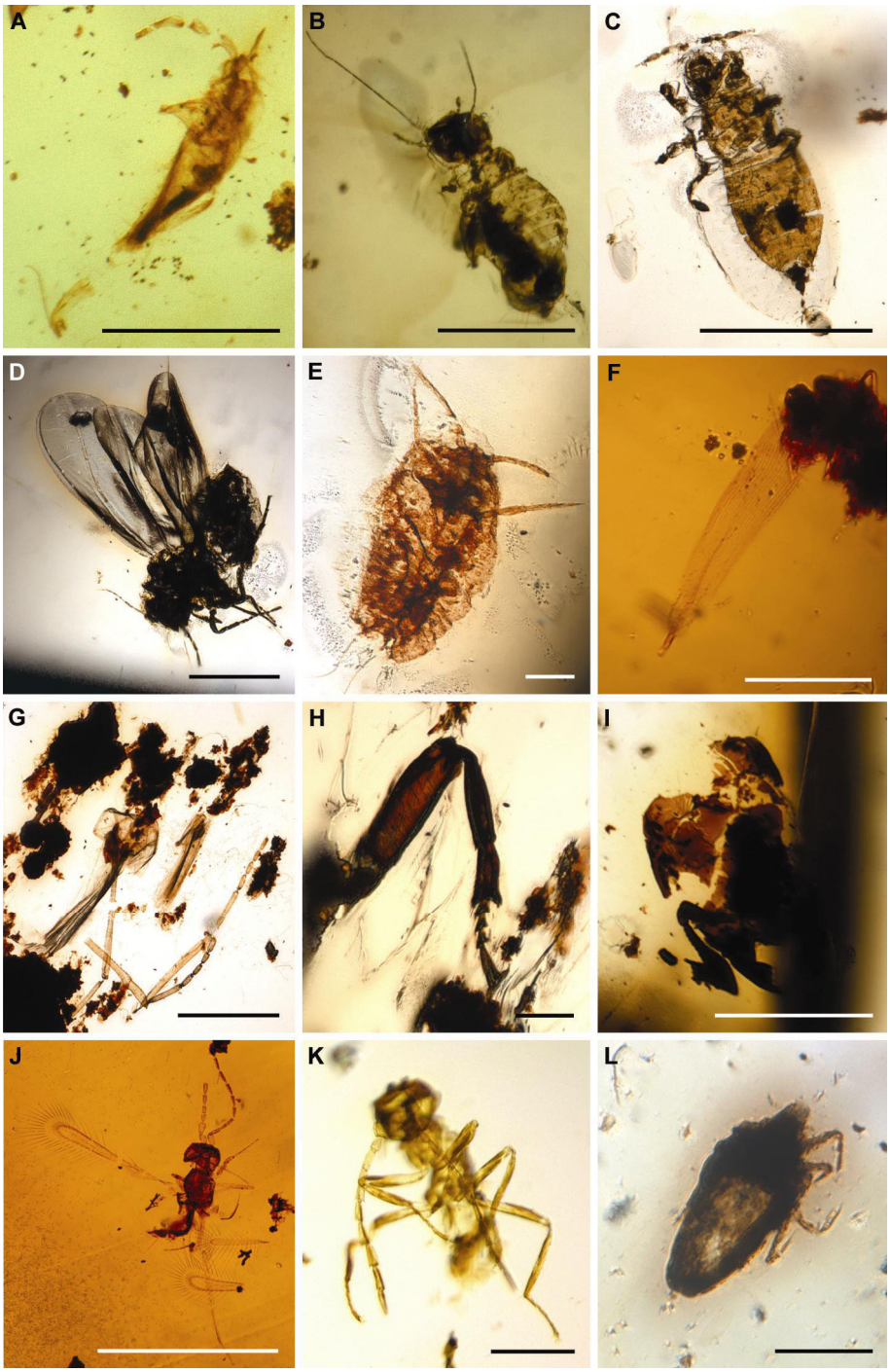

Fig. S10. Further inclusions of arthropods. (*A*) An incomplete springtail (Collembola; NHMW, N6965e). (*B*) An undetermined bark louse larva (Psocoptera; MB. I 5655). (*C*) An undetermined, wingless thrips (Thysanoptera; NHMW, N6967a). (*D*) An undetermined whitefly (Hemiptera: Aleyrodoidea; NHMW, N6973a). (*E*) An undetermined hemipteran larva (NHMW, N6983a). (*F*) A microscopic scale of Lepidoptera (MB. Pb. 2009/204). (*G*) Remnant legs of an undetermined Diptera (NHMW, N6967f). (*H*) Unidentifiable leg of a Coleoptera (NHMW, N6967e). (*I*) Remnant of a head assignable to Coleoptera (NHMW, N6983c). (*J*) An incomplete mymarid wasp (Hymenoptera; MB. I 5654). (*K*) A wingless male mymarid wasp (NHMW, N6980). (*L*) An undetermined mite (Acari; NHMW, N6965h). [Scale bars: 500 µm (*A*–*D*, *G*, *I*, and *J*), and 100 µm (*E*, *F*, *H*, *K*, and *I*).]

Table S1 List of arthropods found in Ethiopian amber

Class Order	Family	#	Collection nº	Figures
Arachnida				
Araneae	Linyphiidae	1	MB. A 1664	Fig. 3*B*
Acari	indet.	2	NHMW N6965h,	Fig. S10*L*
			MB. Pb. 2009/204	–
Entognatha				
Collembola	Isotomidae	1	NHMW, N6969	Fig. 3*D*
	indet.	4	NHMW, N6965d–g	Fig. S10*A*
Insecta				
Zoraptera	indet.	1	NHMW, N6991	Fig. 3*E*
Psocoptera	indet.	1	MB. I 5655	Fig. S10*B*
	indet.	1	NHMW, N6965c	–
Thysanoptera	Merothripidae	1	NHMW, N6974a	Fig. 3*C*
	indet.	1	NHMW, N6967a	Fig. S10*C*
Hemiptera	Aleyrodoidea	1	NHMW, N6973a	Fig. S10*D*
	indet. (larva)	1	NHMW, N6983a	Fig. S10*E*
Lepidoptera	indet. (scales)	1	MB. Pb. 2009/204	Fig. S10*F*
Coleoptera	indet. (head + leg)	1	NHMW, N6967e,	Fig. S10 *H* and *I*
			NHMW, N6983c	
Hymenoptera	Formicidae	1	NHMW, N6976	Fig. 3*A*
	Mymarommatidae	1	NHMW, N6965a	Fig. 3*H*
	Eulophidae	1	NHMW, N6966a	Fig. 3*F*
	Mymaridae	6	NHMW, N6967b,	–
			NHMW, N6970,	–
			NHMW, N6971a–b,	Fig. 3*G*,
			NHMW, N6980,	Fig. S10 *J* and *K*
			MB. I 5654	–
	Trichogrammatidae	1	MB. I 5654	Fig. 3*I*
Diptera	indet. (legs)	1	NHMW, N6967f	Fig. S10*G*
Indet.		2	NHMW, N6965b,	–
			MB. I 5656	–
TOTAL, ARTHROPODS		30		

Bacteria. Abundant branched prokaryotic filaments are found, with filaments up to 1.5 mm in length (Fig. S11 *A–C*). The single cells are rod-shaped, 1.5–5 µm in length and 1–1.5 µm in diameter. Random orientation of the filaments indicates that these prokaryotes grew from their original substrate (detritus including dead arthropods) into the liquid resin. Growth of bacteria into fresh tree resin has been reported from modern *Pinus* resin (67) and postulated for other amber-preserved bacteria (68).

Parasitic fungi. The numerous *Curvularia*-like fungal conidia are obtuse, slightly curved, mostly four-celled, and 8–30 x 6–8.5 µm in size (Fig. 2*C*, Fig. S11 *F* and *G*). The conidiophores of the fungus consist of dark brown, wall-pigmented branched hyphae of up to 1.8 mm length and 6–10 µm diameter (Fig. S11*E*). These hyphae possess short lateral geniculate protrusions of 5–7 µm length, representing the attachment sites of the conidia. The fossil spores are attached to surfaces of successive resin flows in the amber pieces, indicating that they dropped down onto the liquid resin. The plethora of conidia and the occurrence of the related conidiophores in the amber (Fig. S11*E*) suggest that this Cretaceous *Curvularia*-like species sporulated plentifully at the site of the resin-bearing trees. Conidia and fragments of hyphae are the main content of the fecal pellets inside the amber that are up to 800 x 250 µm size (Fig. 2*C* and Fig. S11 *G–I*). Some further fungal remains inside the fecal pellets probably belong to the teleomorphic stage of this *Curvularia*-like fungus (Fig. S11 *H* and *I*). Several tapered and apically obtuse setae are 25–135 µm in length. The setae inside the fecal pellets cannot be assigned to a particular taxon; however, the teleomorphs of *Curvularia* and related genera possess setae of various shapes (69–71). Flat structures of c. 40–75 x 25–40 µm size are also found inside the fecal pellets (Fig. S11*I*). One seta is attached to one of these platelets. The dark brown flat structures inside the pellets are probably fragments of the wall structures of the ascomata, but it is also possible that these structures belong to stromata structures, since similar structures are illustrated from Recent *Cochliobolus* and *Curvularia* species (69, 72, and 73).

Epiphytic fungi. The fragments of the aerial hyphae of sooty moulds found in the Ethiopian amber are up to 130 µm long and the cells are 15–18 x 13 x 17 µm in size (Fig. S11 *J–L*). The rough surface of the globose cells indicates that the inclusions do not belong to the Metacapnodiaceae family reported from Eocene and Oligocene ambers (74); rather, they resemble some representatives of the extant family Antennulariellaceae that possess similar roughened aerial hyphae (75).

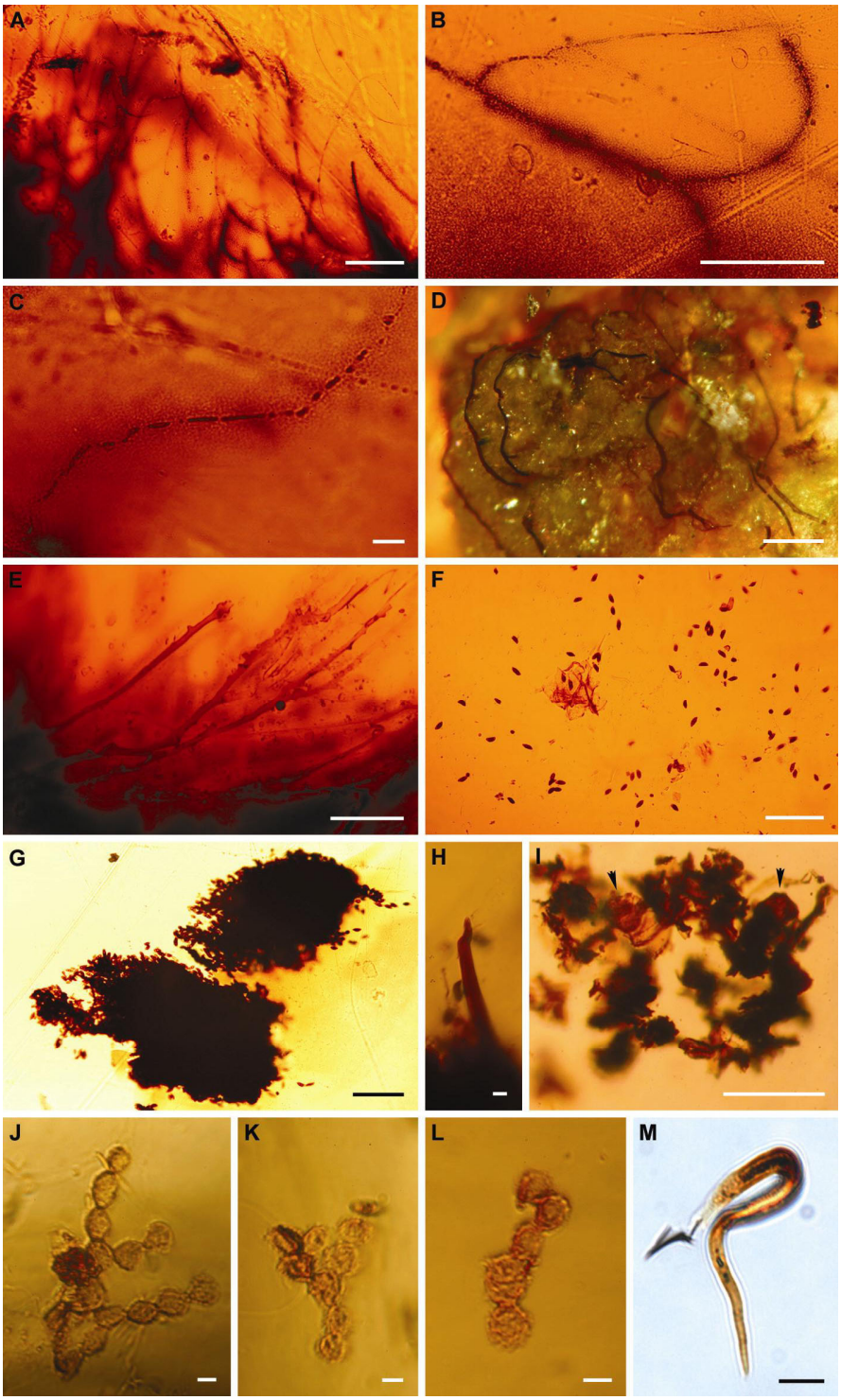

Fig. S11. Further inclusions of microorganisms. (*A*–*C*) Bacterial filaments (MB. Pb. 2009/207). (*D*) Fungal hyphae (MB. Pb. 2009/208). (*E*) Conidiophores of a *Curvularia*-like anamorphic fungus (MB. Pb. 2009/200). (*F*) *Curvularia*-like conidia (MB. Pb. 2009/200). (*G*) Insect fecal pellet composed of *Curvularia*-like conidia (MB. Pb. 2009/201). (*H*, *I*) Seta [(*H*), MB. Pb. 2009/202] and flat structures [arrows in (*I*), MB. Pb. 2009/201] inside insect fecal pellets. (*J*–*L*), Aerial hyphae of sooty moulds resembling the extant Antennulariellaceae (MB. Pb. 2009/204). (*M*) Curved Nematode (NHMW, N6974b). [Scale bars: 100 µm (*A*, *B*, *E*–*G*, *I*); and 10 µm (*C*, *H*, *J*–*M*).]

Stellate hairs of ferns. Stellate pubescence protects young leaves, buds and twigs by effectively preventing evaporation by wind and direct sunlight. Stellate hairs occur in several angiosperm families belonging to euasterids or eurosids, e.g. Brassiciaceae, Capfrifoliacae, Fagaceae, Hydrangaceae, Malvaceae, Meliaceae, Scrophulariaceae, and Tiliaceae, but also in several families of ferns (76, 77). These families belong to lineages of very different origin, including two families of post-K/Pg origin, the Polypodiaceae and Thelypteridacaee, and three lineages that likely originated before the Cretaceous, the Cyatheaceaee, Hymenophyllaceae, and Gleicheniaceae. In ferns, these hairs can be found on the shoot (rhizome) and/or the leaves. The stellate hairs of the Ethiopian amber are well-distinguished from the stellate hairs of oaks (Fagaceae) that are typical inclusions in Paleogene Baltic and Bitterfeld ambers (78). The Cretaceous specimens are more variable in size and in the number of the single hairs (rays). All other investigated stellate hairs of angiosperms possess rays that are roundish in diameter, not flat as in our fossils.

In one type of stellate hair, the single hairs are arranged from a common point (at which the sessile hairs were attached to the leaf surface) and spread in many directions, forming stellate tufts (Fig. 2*D*, Fig. S12 *D–F*). The size of these composed hairs ranges from 240 to 800 µm. The number of elongate and slightly tapered single hairs in a tuft varies from 8 to 26. These hairs most likely derive from tree ferns of the family Cyatheaceae; such hairs can be found in various modern species of this family. Tree ferns are a common plant in tropical mountain forests. Another type of stellate hairs is flat and has only eight single rays that are also flat but thin and almost filiform (Fig. 2*E*). These hairs are 550 to 880 µm in diameter. Similarly composed hairs are found in extant species of the genera *Hymenophyllum* and *Trichomanes* belonging to the species-rich filmy fern family, Hymenophyllaceae that frequently grow epiphytic but also terrestrial or saxicolous.

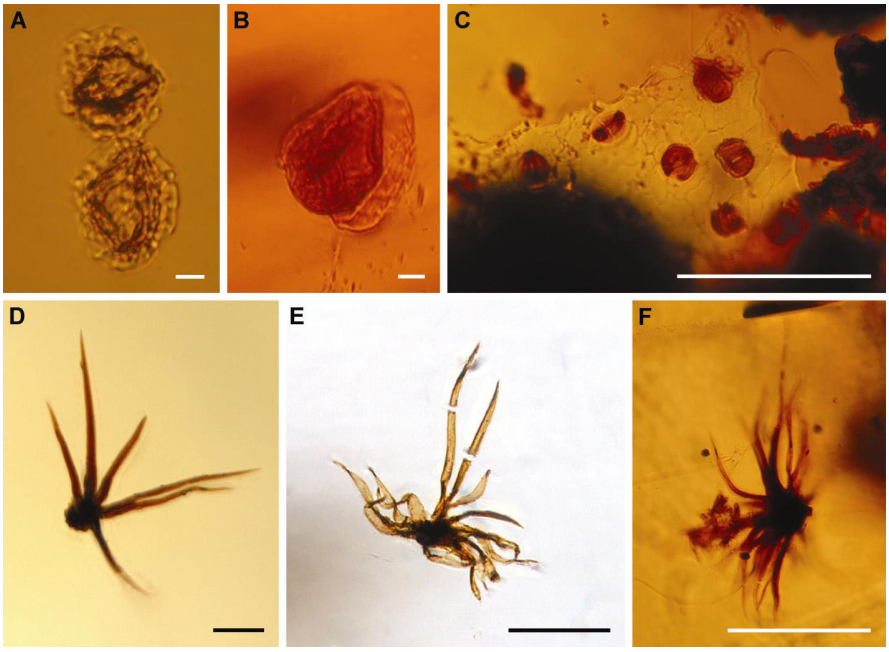

Fig. S12. Further amber inclusions of plant remnants. (*A*) Spores of Lycopodiaceae (NHMW, N6964). (*B*) Saccate pollen grain of a Podocarpaceae representative (MB. Pb. 2009/200). (*C*) Cuticle from an angiosperm with putative relationship either to Lauraceae, Chloranthaceae or Proteaceae (MB. Pb. 2009/209). (*D–F*), Stellate hairs resembling those of modern representatives of the tree-fern family *Cyatheaceae* [(*D*), NHMW, N6966b; (*E*), NHMW, N6973b; (*F*), MB. Pb. 2009/202]. [Scale bars: 10 µm (*A*, *B*), and 100 µm (*C–F*).]

1. Blakey RC (2009) Global Paleogeography, Mollewide Globes, Late Early Cretaceous (105Ma), http://jan.ucc.nau.edu/~rcb7/105moll.jpg.
2. Martínez-Delclòs X, Briggs DEG, Peñalver E (2004) Taphonomy of insects in carbonates and amber. *Palaeogeogr Palaeoclimat Palaeoecol* 203:19–64 .
3. Pereira R, Carvalho IS, Simoneit BRT, Azevedo DA (2009) Molecular composition and chemosystematic aspects of Cretaceous amber from the Amazonas, Araripe and Recôncavo basins, Brazil. *Org Geochem* 40:863–875.
4. Perrichot V, Néraudeau D, Nel A, de Ploëg G (2007) A reassessment of the Cretaceous amber deposits from France and their palaeontological significance. *Afr Invertebr* 48:213–227.
5. Gomez B, Barale G, Saad D, Perrichot V (2003) Santonian angiosperm-dominated leaf-assemblage from Piolenc (Vaucluse, SE France). *C R Palevol* 2:197–204.
6. Guiliano M, Mille G, Onoratini G, Simon P (2006) Presence of amber in the Upper Cretaceous (Santonian) of 'La Mède' (Martigues, southeastern France). IRTF characterization. *C R Palevol* 5:851–858 (in French).
7. Bingham PS, Savrda CE, Knight TK, Lewis RD (2008) Character and genesis of the Ingersoll Shale, a compact continental Fossil-Lagerstätte, Upper Cretaceous Eutaw Formation, Eastern Alabama. *Palaios* 23:391–401.
8. Russo A, Assefa G, Atnafu B (1994) Sedimentary evolution of the Abay River (Blue Nil) Basin, Ethiopia. *Neues Jahrb Geol P-M* 1994/5:291–308.
9. Assefa G (1991) Lithostratigraphy and environment of deposition of the Late Jurassic – Early Cretaceous sequence of the central part of the Northwestern Plateau, Ethiopia. *Neues Jahrb Geol P-A* 182:255–284.
10. Goodwin MB, *et al*. (1999) Mesozoic continental vertebrates with associated palynostratigraphic dates from the northwestern Ethiopian Plateau. *J Vertebr Paleontol* 19:728–741.
11. Bosellini A, Russo A, Assefa G (2001) The Mesozoic succession of Dire Dawa, Harar Province, Ethiopia. *J Afr Earth Sci* 32:403–417.
12. Perrichot V (2005) Amber- and plant-bearing paralic environments from the Cretaceous of northern Aquitain (Charentes, southwestern France). *Mém Géosciences Rennes* 118:1–310 (in French).
13. Wimmer R, Pester L, Eissmann L (2006) The amber-bearing Tertiary between Leipzig and Bitterfeld. *Mauritiana (Altenburg)* 19:373–421 (in German).
14. Anderson KB, Winans RE (1991) The Nature and Fate of Natural Resins in the Geosphere. I. Evaluation of Pyrolysis-Gas Chromatography-Mass Spectrometry for the Analysis of Plant Resins and Resinites. *Anal Chem* 63:2901–2908.
15. Anderson KB (2006) The nature and fate of natural resins in the geosphere. XII. Investigation of C-ring aromatic diterpenoids in Raritan amber by pyrolysis-GC-matrix isolation FTIR-MS. *Geochem Trans* 7:2.
16. Nascimbene P, Biscula C, Grimaldi DA (2007) Physical properties of amber: an analysis and comparison of the density and hardness of samples from various ages and localities. *Abstract Volume, the FossilsX3 Congress: Insects, Arthropods, Amber* (Vitoria-Gasteiz), p 228.
17. Currie SJA (1997) A study of New Zealand Kauri copal. *J Gemmol* 25:408–416.
18. Langenheim JH, Beck CW (1968) Catalogue of infrared spectra of fossil resins (ambers): I. North and South America. *Bot Mus Leaf Harv Univ* 22:65–120.
19. Broughton PL (1974) Conceptual frameworks for geographic–botanical affinities of fossil resins. *Can J Earth Sci* 11:583–594.

20. Beck CW, Wilbur E, Meret S, Kossove D, Kermani, K (1966) Infrared spectra and the origin of amber. *Archaeometry* 9:96–108.
21. Vávra N, Vycudilik W (1976) Chemical investigations of fossil and subfossil resins. *Beitr Paläont Österr* 1:121–135 (in German).
22. Tonidandel L, Ragazzi E, Traldi P (2009) Mass spectrometry in the characterization of Ambers. II. Free succinic acid in fossil resins of different origin. *Rapid Commun Mass Sp* 23:403–408.
23. Beck CW, Wilbur E, Meret S (1964) Infra-red spectra and the origin of amber. *Nature* 201:256–257.
24. Langenheim JH, Beck CW (1965) Infrared spectra as a means of determining botanical sources of amber. *Science* 149:52–55.
25. Beck CW (1986) Spectroscopic investigations on amber. *Appl Spectrosc Rev* 22:57–110.
26. Kosmowska-Ceranowicz B (1999) Succinite and some other fossil resins in Poland and Europe (deposits, finds, features and differences in IRS). *Estud Mus Cienc Àlava* 14:73–117.
27. Matuszewska A, Karwowski L (1999) Physicochemical analysis of the molecular and macromolecular phases of Baltic amber. *Estud Mus Cienc Àlava* 14:49–62.
28. Poinar GO Jr (1991) *Hymenaea protera* sp. n. (Leguminosae, Caesalpinioideae) from Dominican amber has African affinities. *Experientia* 47:1075–1082.
29. Poinar GO Jr, Brown AE (2002) *Hymenaea mexicana* sp. nov. (Leguminosae: Caesalpinioideae) from Mexican amber indicates Old World connections. *Bot J Linn Soc* 139:125–132.
30. Langenheim JH (1969) Amber: a botanical inquiry. *Science* 163:1157–1169.
31. Beck CW (1999) The chemistry of amber. *Estud Mus Cienc Àlava* 14:33–48.
32. Wolfe AP, *et al*. (2009) A new proposal concerning the botanical origin of Baltic amber. *Proc Roy Soc Biol Sci* 276:3403–3412.
33. Alonso JA, *et al.* (2000) A new fossil resin with biological inclusions in Lower Cretaceous deposits from Álava (Northern Spain, Basque-Cantabrian Basin) *J Paleontol* 74:158–177.
34. Roghi G, Ragazzi E, Gianolla P (2006) Triassic Amber of the Southern Alps (Italy) *Palaios* 21:143–154.
35. Anderson KB, Winans RE, Botto RE (1992) The nature and fate of natural resins in the geosphere: II. Identification, classification and nomenclature of resinites. *Org Geochem* 18:829–841.
36. Rodgers KA, Currie S (1999) A thermal analytical study of some modern and fossil resins from New Zealand. *Thermochim Acta* 326:143–149.
37. Ragazzi E, Roghi G, Giaretta A, Gianolla P (2003) Classification of amber based on thermal analysis. *Thermochim Acta* 404:43–54.
38. Ragazzi E, *et al*. (2009) Thermal analysis of Cretaceous ambers from southern France. *Geodiversitas* 31:163–175.
39. Langenheim JH (1995) The biology of amber-producing trees: focus on case studies of *Hymenaea* and *Agathis*. *ACS Sym Ser* 617:1–31.
40. Bray PS, Anderson KB (2009) Identification of Carboniferous (320 Million Years Old) Class Ic amber. *Science* 326:132.
41. Anderson KB (1995) The Nature and Fate of Natural Resins in the Geosphere. V. New Evidence Concerning the Structure, Composition and Maturation of Class I (Polylabdanoid) Resinites. *ACS Sym Ser* 617:105–129.

42. Jarzen DM, Elsik WC (1986) Fungal palynomorphs recovered from recent river deposits, Luangwa Valley, Zambia. *Palynology* 10:35–60.
43. Schrank E (1994) Nonmarine Cretaceous palynology of the northern Kordofan, Sudan, with notes on fossil Salviniales (water ferns). *Geol Rundsch* 83:773–786.
44. Herngreen GFA, Chlonova AF (1981) Cretaceous microfloral provinces. *Pollen et Spores* 23:441–555.
45. Schrank E (1991) Mesozoic palynology and continental sdiments in NE Africa (Egypt and Sudan) – a review. *J Afr Earth Sci* 12:363–373.
46. Ansorge J (2007) Upper Triassic insects and amber from Lesotho (South Africa). *Abstract Volume, the FossilsX3 Congress: Insects, Arthropods, Amber* (Vitoria-Gasteiz), pp 52–54.
47. Gomez B, Martinez-Delclos X, Bamford M, Philippe M (2002) Taphonomy and palaeoecology of plant remains from the oldest African Early Cretaceous amber locality. *Lethaia* 35:300–308.
48. Schlüter T, von Gnielinski F (1987) The East African copal - Its geologic, stratigraphic, palaeontologic significance and comparison with other fossil resins of similar age. *National Museums of Tanzania Occasional Paper* 8:1–32.
49. Nissenbaum A, Horowitz A (1992) The Levantine amber belt. *J Afr Earth Sci* 14:295–300.
50. Poinar GO Jr, Milki R (2001) *Lebanese Amber. The Oldest Insect Ecosystem in Fossilized Resin* (Oregon State Univ. Press, Corvallis).
51. Azar D (2000) *Mesozoic Lebanese Ambers*. Ph.D. Thesis, 164 p. University Paris XI-Orsay, Paris (in French).
52. Langenheim JH (2003) *Plant Resins: Chemistry, Evolution, Ecology and Ethnobotany* (Timber Press, Portland).
53. Krumbiegel G, Krumbiegel B (2005) *Amber – Fossil Resins from all over the World* (Quelle & Meyer, Wiebelsheim, in German).
54. Brothers DJ, Rasnitsyn AP (2003) Diversity of Hymenoptera and other insects in the Late Cretaceous (Turonian) deposits at Orapa, Botswana: a preliminary review. *Afr Entomol* 11:221–226.
55. Nel A, Zarbout M, Barale G, Philippe M (1998) *Liassotettigarcta africana* sp. n. (Auchenorrhyncha: Cicadoidea: Tettigarctidae), the first Mesozoic insect from Tunisia. *Eur J Entomol* 95:593–598.
56. Schlüter T (2003) Fossil insects in Gondwana - localities and palaeodiversity trends. *Acta Zool Cracov* 46:345–371.
57. Mound LA, O'Neill K (1974) Taxonomy of the Merothripidae, with ecological and phylogenetic considerations (Insecta: Thysanoptera). *J Nat Hist* 8:481–509.
58. zur Strassen R (1973) Insect fossils from the Early Cretaceous - 5. Fossil Thysanoptera from Mesozoic Lebanese amber (Insecta: Thysanoptera). *Stutt Beitr Naturk-A* 256:1–51 (in German).
59. Bhatti JS (1979) A revised classification of Thysanoptera. *Abstract Volume, the Workshop on Advances in Insect Taxonomy in India and the Orient (Manali)*, pp 46–48.
60. Priesner H (1929) Amber-Thysanoptera II. *Bernstein-Forschungen* 1:111–138 (in German).
61. Engel MS (2004) in *Biodiversity, Taxonomy and Biogeography of Arthropods from Mexico: Towards a Synthesys of our Knowledge*, eds Bousquets JL, Morrone JJ,

Ordóñez OY, Fernández IV (Universidad Nacional Autónoma de México, México) pp 175–186.
62. Arnedo MA, Scharff N, Hormiga G (2009) Higher level phylogenetics of linyphiid spiders (Araneae, Linyphiidae) based on morphological and molecular evidence. *Cladistics* 25:231–262.
63. Viggiani G (1971) Research on chalcidoid Hymenoptera. XXVIII. Comparative morphological study of the external male genitalia in the Trichogrammatidae. *Boll Lab Entomol Agraria* 29:181–222 (in Italian).
64. Tafforeau P, *et al*. (2006) Applications of X-ray synchrotron microtomography for non-destructive 3D studies of paleontological specimens. *App Phys A-Mater* 83:195–202.
65. Lak M, *et al*. (2008) Phase contrast X-ray synchrotron imaging: opening access to fossil inclusions in opaque amber. *Microsc Microanal* 14:251–259.
66. Dlussky GM, Brothers DJ, Rasnitsyn AP (2004) The first Late Cretaceous ants (Hymenoptera : Formicidae) from southern Africa, with comments on the origin of the Myrmicinae. *Insect Syst Evol* 35:1–13.
67. Schmidt AR, Dilcher DL (2007) Aquatic organisms as amber inclusions and examples from a modern swamp forest. *Proc Natl Acad Sci USA* 104:16581–16585.
68. Schmidt AR, Schäfer U (2005) *Leptotrichites resinatus* new genus and species, a fossil sheathed bacterium in alpine Cretaceous amber. *J Paleontol* 79:184–193.
69. Alcorn JL (1990) Additions to *Bipolaris*, *Cochliobolus* and *Curvularia*. *Mycotaxon* 39:361–392.
70. Tsuda M, Ueyama, A (1977) *Pseudocochliobolus nisikadoi*, the perfect state of *Helminthosporium coicis*. *Mycologia* 69:1109–1120.
71. Drechsler C (1934) Phytopathological and taxonomic aspects of *Ophiobolus*, *Pyrenophora*, *Helmithosporium* and a new genus, *Cochliobolus*. *Phytopathology* 24:953–983.
72. Nelson RR (1964) The perfect stage of *Curvularia geniculata*. *Mycologia* 56:777–779.
73. Ellis MB (1966) Dematiaceous Hyphomycetes VII: *Curvularia*, *Brachysporium*, etc. *Mycol Papers* 106:1–57.
74. Rikkinen J, Dörfelt H, Schmidt AR, Wunderlich J (2003) Sooty moulds from European Tertiary amber, with notes on the systematic position of *Rosaria* (Cyanobacteria). *Mycol Res* 107:251–256.
75. Hughes SJ (1976) Sooty moulds. *Mycologia* 68:693–820.
76. McCleery EM (1907) Stellate hairs and peltate scales of Ohio plants. *The Ohio Naturalist* 7:51–56.
77. Ogura Y (1938) *Anatomy of the Vegetative Organs of the Pteridophytes* (Bornträger, Berlin, in German).
78. Weitschat W, Wichard W (2002) *Atlas of Plants and Animals in Baltic Amber*. (Pfeil, Munich).